

# How News Evolves? Modeling News Text and Coverage using Graphs and Hawkes Process

1<sup>st</sup> Honggen Zhang

*Electrical and Computer Engineering  
University of Hawai'i at Mānoa  
Honolulu, USA  
honggen@hawaii.edu*

2<sup>nd</sup> June Zhang

*Electrical and Computer Engineering  
University of Hawai'i at Mānoa  
Honolulu, USA  
zjz@hawaii.edu*

**Abstract**—Monitoring news content automatically is an important problem. News content, unlike traditional text, has a temporal component. However, few works have explored the combination of natural language processing and dynamic system models. One reason is that it is challenging to mathematically model the nuances of natural language. In this paper, we discuss how we built a novel dataset of news articles collected over time. Then, we present a method of converting news text collected over time to a sequence of directed multi-graphs, which represent semantic triples (Subject  $\rightarrow$  Predicate  $\rightarrow$  Object). We model the dynamics of specific topological changes from these graphs using discrete-time Hawkes processes. With our real-world data, we show that analyzing the structures of the graphs and the discrete-time Hawkes process model can yield insights on how the news events were covered and how to predict how it may be covered in the future.

**Index Terms**—Temporal Text Mining, semantic representation, event extraction, relation extraction, Hawkes process, graphs, networks

## I. INTRODUCTION

The rise of internet news media generates a lot of news stream. Unlike general text, news text is inherently temporal, comprising of a series of events over time and space. Several problems are associated with the automatic analysis of news text such as event detection, relation detection, and fake news detection. Researchers working in Temporal Text Mining use tools to automatically extract events and to cluster and organize them by temporal relationships. However, these works do not model how the events change over time with a mathematical model.

On the other hand, dynamical information from a mathematical can be very informative in understanding and building features on how events evolve in time. Recently, classifiers to detect fake tweets use a combination of text features and dynamics parameters. The dynamics parameters are obtained by fitting a Hawkes process model to the observed count of tweets and retweets over time. However, Hawkes process has not been used to analyze the evolution of news text.

In this paper, we present a framework of using the discrete-time Hawkes process to model how news coverage of a particular event change over time with the eventual goal of building a normative dynamic model of news coverage and to be able to detect why anomalous news coverage occurs. Figure 1 shows an overview of the framework.

First, we collected news articles from the internet related to specific events using Event Registry. Two events are discussed in this paper: 1) the **Alleged assault of Jussie Smollett** and 2) **Ukraine International Airlines Flight 752 crashed in Iran**. The dataset, collected from 3,145 different news sources, contains 44,403 news articles with the complete raw text, publication time, and metadata information. The dataset is available on Github<sup>1</sup>.

We process the article text with ReVerb [1] to extract semantic triples with the pattern Subject  $\rightarrow$  Predicate  $\rightarrow$  Object. We present the triples using the nodes and edges of a Resource Description Framework (RDF) graph (i.e., directed multi-graph with words and phrases associated with both the nodes and the edges). A stream of news articles can be converted to a sequence of RDF graphs.

The dynamics of how the RDF graphs change over time contain semantic (i.e., what happened), linguistic (i.e., how events were described/interpreted), and coverage (i.e., how many articles were published) information. Because it is very difficult to mathematically model dynamic graphs, we model instead specific topological changes on the graph structure using the Hawkes process.

Section II will review related prior work. We discuss our data collection and cleaning methods in Section III. Section IV details how we transformed text data into a sequence of RDF graphs and finally, a collection multivariate time series. We introduce the discrete-time Hawkes process model and apply it to multivariate time series in Section V. We discuss our experiments in fitting the collected data to the Hawkes process and analysis of the learned parameters in Section VI. We then use the discrete-time Hawkes process for forecasting. We show that our model has comparable performance as other forecasting methods such as VAR [2] and LSTNet [3] but has the additional advantage of being interpretable. Section VII concludes the paper.

## II. RELATED WORK

Works in Temporal Text Mining (TTM) are primarily focused in either event detection or relation detection. Works in event detection focus on automatically finding events from

<sup>1</sup><https://github.com/honggen-zhang/News-Evolve-on-DHP>

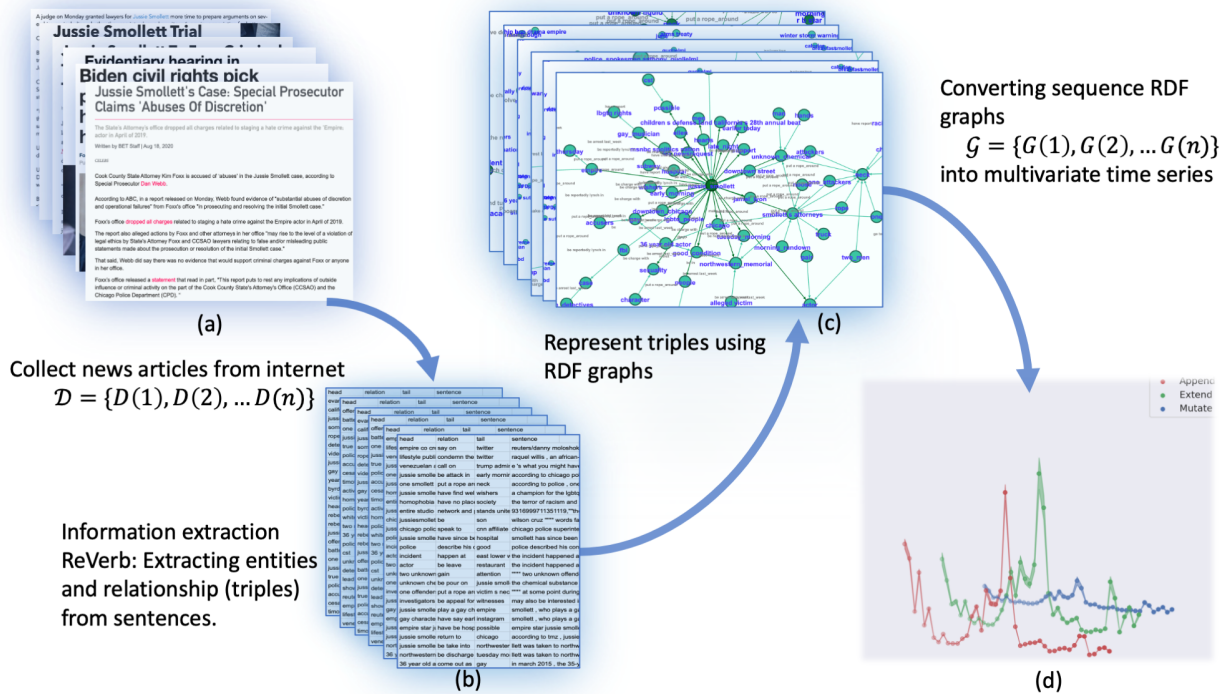


Fig. 1: Proposed Framework.

sets of news articles [4], [5]. In some work, the events are then placed in some sort of temporal order and visualized as a directed graph. In [6], the news articles related to specific events are also automatically summarized. Various clustering methods have been used to gather multiple articles related to a specific event together [7], [8].

Work such as the Event Threading model in [9] and the Story Forest in [10] place more emphasis on discovering the relationships (usually temporal) that connect multiple events together. The temporal relationships are visualized as a directed graph and are used to track the dynamic of events. Works that have used graphs to describe the evolutionary pattern of specific events are [11]–[14]. Usually evolution is characterized by some sort of distance measurement between pairs of events.

### A. Hawkes process

The Hawkes process is a point process whose realization consists of discrete events localized in time [15]. It is a self-exciting process in that the rate of occurrence depends on the history of the process. For example, a history of a high number of occurrences in a short period of time will increase the probability of the event occurring in the near future. Hawkes processes are often used to model time series data with ‘bursty’ dynamics.

Recently, several works have used Hawkes process to build classifiers to detect fake tweets [16], [17]. In Dutta et al.’s HawkesEye classifier [18], dynamics parameters of the learned Hawkes process are combined with semantic information from the text to generate features to train the classifiers.

Reference [16] used the Hawkes process to build a normative model of the dynamics of tweets, which can then be used for anomaly detection.

## III. DATA COLLECTION AND EXTRACTION

We scrapped news articles from the news collection platform Event Registry [19]. The platform provides a useful Python API, so we can download custom news articles by attributes such as keywords, language, place. In this paper, two events were selected, the **Alleged assault of Jussie Smollett** and **Ukraine International Airlines Flight 752 crashed in Iran**. Each news article is scrapped based on specific keywords. Specifically, we used *Jussie Smollett* and *Iran, Plane* as the keywords to obtain two datasets: JS and IP, respectively. The JS dataset contains 11,340 news articles collected from 1,009 news sources spanning January 28, 2019 to March 14, 2019. The IP dataset contains 33,063 news articles collected from 2,136 news sources spanning January 02, 2020 to February 01, 2020. Figure 2 shows the number of articles collected each day. In addition to the extracted raw text, collected articles also contain (if available): 1) URL of article, 2) publication date, 3) title, 4) authors, 5) URL of associated image, 6) keywords.

### A. Text to Triples to Graph Representation

We needed to extract the semantic information from the article text. We used ReVerb [1] to extract semantic triples in the form  $Head(h) \rightarrow Relation(r) \rightarrow Tail(t)$ . For example, the triple Barack Obama  $\rightarrow$  born in  $\rightarrow$  Honolulu can be extracted from the sentence *Barack Obama was born in Honolulu*.

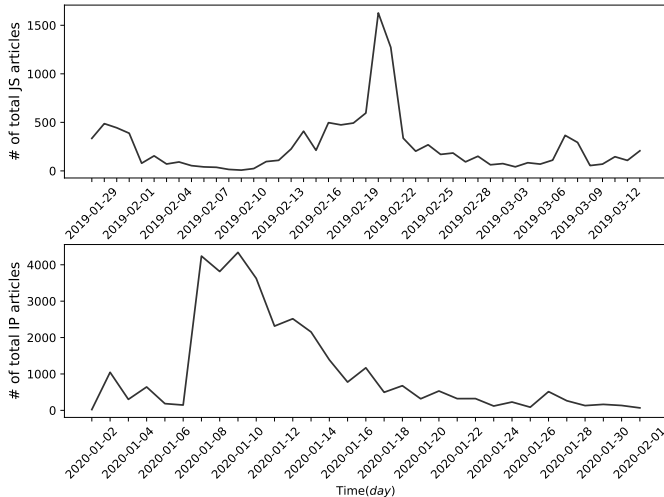


Fig. 2: Number of Articles Collected per Day of Dataset JS and Dataset IP

Reverb extracts triples from syntactic constraints based on verb phrases. Therefore, multiple triples may be extracted from a single sentence. Triples follow the basic Subject  $\rightarrow$  Predicate  $\rightarrow$  Object pattern of English. Triples were also used in [12] to help extract events.

We can collect a set triples into a directed multigraph where the nodes correspond to the Head and Tail phrases of the triple and the edges correspond to the Relation phrase of the triple. Because multiple relations can exist between the same Head and Tail phrases, multiple edges can exist between a pair of nodes. In this paper, we will refer to such a graph constructed from semantic triples as an RDF (Resource Description Framework) graph due to the similarities in structure.

### B. Data Cleaning

Substantive efforts were put into cleaning the extracted triples. Some of the issues we encountered: 1) ambiguous pronoun references, 2) duplicate entities references such as *U.S.* and *America*. For the first problem, we used the co-reference tool NeuralCoref [20] provided in Spacy [21]. For the second problem, we devised a multiple way of computing similarity between phrases to detect semantic duplication.

First, we determined duplication between phrases by counting the number of overlap words; we refer to this as coarse similarity. Let  $P_1$  and  $P_2$  be two phrases of interest. The coarse similarity distance between  $P_1$  and  $P_2$  is

$$\frac{|P_1 \cap P_2|}{\max(|P_1|, |P_2|)},$$

where  $|P_i|$  is the total number of words in the  $i$ th phrase and  $|P_1 \cap P_2|$  is the number of words that occurred in both phrases. Thresholding the coarse similarity distance will help to associate phrases such as *social media*, *social medias posts*, and *social medias platform* together.

Next, we project the words in two different phrases into embedding space using Word2Vec [22]; we refer to this as

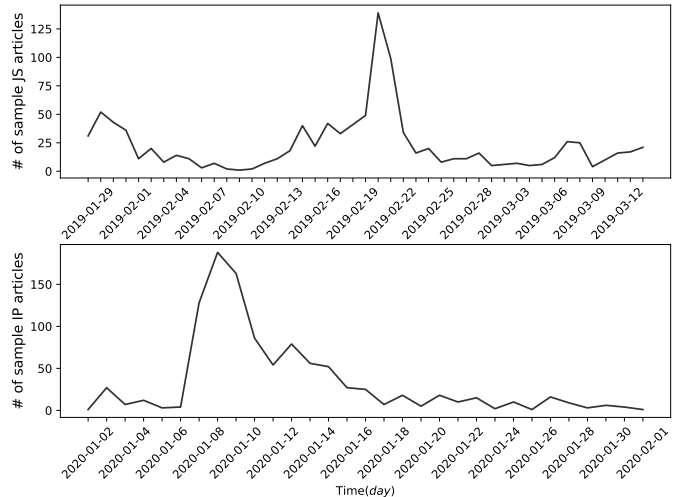


Fig. 3: Number of Sample Articles per Day of Dataset JS and Dataset IP

fine similarity. The fine similarity distance between  $P_1$  and  $P_2$  is

$$\frac{\sum_{w_1 \in P_1} \sum_{w_2 \in P_2} \cos(w_1, w_2)}{|P_1| + |P_2|},$$

where  $\cos(w_1, w_2)$  is the cosine distance between the embedded vector representation of words in  $P_1$  and  $P_2$ . By thresholding the fine similarity distance can help to connect related but seemingly dissimilar phrases such as *emperor actor* and *jussie smollett* together.

We applied the cleaning process to the nodes and edges of the RDF graph. Due to the computational cost of having to compare every pair of phrases, we randomly sampled 27-30 news sources for a total of approximately 1,000 articles from each dataset. We can see from Figure 3 that the randomly sampled articles has similar dynamics to entire dataset (see Figure 2).

## IV. PROBLEM FORMULATION

Given a set of articles on a specific news event over time,  $D = \{D(1), \dots, D(N)\}$ , where  $D(n)$  is the set of all the news articles collected on day  $n$ . Our goal is to develop a dynamic model of  $D$  that includes 1) the semantic information contained in the articles and 2) the dynamic of news coverage (i.e., number of articles written on the topic per day). We transform the text data  $D = \{D(1), \dots, D(N)\}$  into a sequence of RDF graphs  $\mathcal{G} = \{G(1), \dots, G(N)\}$  consisting of semantic triples extracted from  $D(n)$ . Our goal is then to describe the dynamics of  $\mathcal{G}$ .

Directly modeling the dynamics of a directed, multigraph is mathematically difficult due to the combinatorial-sized state space. Instead, we can consider how substructures (i.e., triples) of  $\mathcal{G}$  changes overtime.

Let  $\mathbf{G}_n^{n+m}$  denote the cumulative RDF graph from day  $n$  to day  $n + m$ :

$$\mathbf{G}_n^{n+m} = G(n) \cup G(n+1) \cup \dots \cup G(n+m).$$

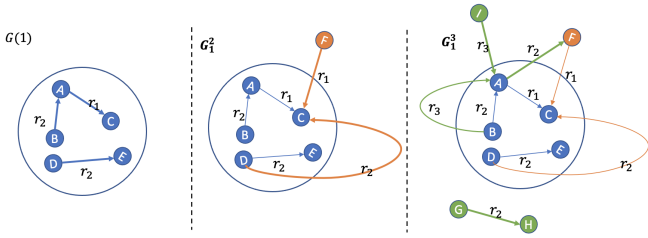


Fig. 4: Example RDF Graph Sequence (Red = New Triples on Day 2, Green = New Triples on Day 3)

We can consider how a new graph (i.e. set triples) on day  $n+1$ ,  $G(n+1)$ , may differ from the previous days graphs  $G_1^n$ . In this paper, we consider three types of structural changes to  $G_1^n$ :

- Append:** A new triple of  $G(n+1)$  either appends to the head or tail of a triple in  $G_1^n$ . New nodes and edges appear in  $G_1^{n+1}$  when append occurs. From a semantic perspective, occurrences of append events imply that new articles are presenting sentences/information that was unseen before.
- Extend:** A new triple of  $G(n+1)$  connects two disconnected triples in  $G_1^n$ . Graph  $G_1^{n+1}$  have additional edges and become more connected when extend occurs. From a semantic perspective, occurrences of extend events imply that connections are drawn between previous concepts.
- Mutate:** A new triple of  $G(n+1)$  have the same head and tail as a triple in  $G_1^n$  but a different relationship. mutate events does not change the structure  $G_1^{n+1}$  if we discount multiple edges. From a semantic perspective, occurrences of mutate events imply that alternative interpretation/wordings are presented.

Figure 4 shows an example illustrating how the cumulative RDF graphs grows from  $G(1)$  to  $G_1^3$ . The initial set of triples in  $G(1)$  are  $A \rightarrow r_1 \rightarrow C$ ,  $B \rightarrow r_2 \rightarrow A$ , and  $D \rightarrow r_2 \rightarrow E$ . We will track what happens to these initial triples over time.

- On day 2, the new triple  $F \rightarrow r_1 \rightarrow C$  appends to the initial triple  $A \rightarrow r_1 \rightarrow C$  and the new triple  $D \rightarrow r_2 \rightarrow C$  is an extension of  $A \rightarrow r_1 \rightarrow C$ . On day 3, the new triple  $I \rightarrow r_3 \rightarrow A$  appends to  $A \rightarrow r_1 \rightarrow C$ . Two new triples,  $A \rightarrow r_2 \rightarrow F$ ,  $B \rightarrow r_3 \rightarrow A$ , are extensions of  $A \rightarrow r_1 \rightarrow C$
- On day 2, the initial triple  $B \rightarrow r_2 \rightarrow A$  is unchanged. On day 3, the new triple  $B \rightarrow r_3 \rightarrow A$  is a mutation of  $B \rightarrow r_2 \rightarrow A$ ,  $I \rightarrow r_3 \rightarrow A$  appends to  $B \rightarrow r_2 \rightarrow A$  and  $A \rightarrow r_2 \rightarrow F$  are extensions of  $B \rightarrow r_2 \rightarrow A$ .
- On day 2, the new triple  $D \rightarrow r_2 \rightarrow C$  is an extension of the initial triple  $D \rightarrow r_2 \rightarrow E$ . On day 3,  $D \rightarrow r_2 \rightarrow E$  is unchanged.

By keeping track of the append, extend, mutate events, we can characterize how the cumulative RDF graph changes over time. Let  $\mathcal{I}$  denote the initial set of triples. Each triple in  $\mathcal{I}$

induces a multivariate time series over time:

$$\mathbf{y}^{(i)}(n) = \begin{bmatrix} y_{\text{append}}^{(i)}(n) \\ y_{\text{extend}}^{(i)}(n) \\ y_{\text{mutate}}^{(i)}(n) \end{bmatrix}, i \in \mathcal{I}, n = 1, \dots, N, \quad (1)$$

where  $y_{\text{append}}^{(i)}(n)$  is the total number of new triples on day  $n$  that are appended to triple  $i$ ;  $y_{\text{extend}}^{(i)}(n)$  is the total number of new triples on day  $n$  that are extension of  $i$ , and  $y_{\text{mutate}}^{(i)}(n)$  is the total number of triples on day  $n$  that are mutations of  $i$ .

The problem of characterizing the evolution of  $D(n)$  by way of accounting for the structural changes of the cumulative RDF graph  $G_1^N$  can be done by fitting a model to  $\{\mathbf{y}^{(1)}(n), \mathbf{y}^{(2)}(n), \dots, \mathbf{y}^{(|\mathcal{I}|)}(n)\}$ .

## V. DISCRETE-TIME HAWKES PROCESS

The classic Hawkes process is a continuous-time model. This means that event cannot occur simultaneously; this is a reasonable assumption for a continuous-time system. However, our data was collected per day. Therefore, it is very likely that multiple events occurred in the same day and the data could not be modeled by a continuous-time process. In this paper, we used the discrete-time variation of the Hawkes process, introduced in [23] to model induced the time series.

Consider a discrete-time Hawkes process,  $\mathbf{y}(n) = [y_1(n), \dots, y_M(n)]^T$ , where  $y_m(n)$  represents the number of occurrences of the  $m$ th type of event in the  $n$ th time interval. Let  $\mathbf{H}_1^{n-1} = \{\mathbf{y}(1), \dots, \mathbf{y}(n-1)\}$  denote the history of the process up to time interval  $n-1$ . The discrete-time Hawkes process is characterized by the conditional intensity function

$$\lambda(n) = E[\mathbf{y}(n) | \mathbf{H}_1^{n-1}] = \mu + \sum_{t < n} \mathbf{A} \mathbf{y}(t) \phi(n-t), \quad (2)$$

where  $\mu = [\mu_1, \dots, \mu_M]^T$  is the baseline vector. And  $A$  is the  $M \times M$  infectivity matrix where  $A_{ij}$  shows how the  $i$ th event type is influenced by the  $j$ th event type. The function  $\phi(t)$  is the delay function. A popular delay function is the exponential function:

$$\phi(t) := \beta e^{-\beta t}, t \geq 0. \quad (3)$$

According to the discrete-time Hawkes process, each time-series  $y_m(n)$  is an inhomogeneous Poisson process with rate  $\lambda_m(n)$ .

$$P(y_m(n); \lambda_m(n)) = \frac{(\lambda_m(n))^{y_m(n)}}{y_m(n)!} e^{-\lambda_m(n)}, \quad 1 \leq m \leq M. \quad (4)$$

### A. Parameter Estimation

The parameters of the discrete-time, multivariate Hawkes process are  $\Theta = \{\mu, A\}$ . The parameter  $\beta$  of the delay function is a hyperparameter. We will estimate  $\Theta$  using maximum likelihood:

$$\hat{\Theta} = \arg \max_{\Theta} \mathcal{L}(\Theta),$$

where the log-likelihood function is

$$\begin{aligned} \mathcal{L}(\Theta) &= \log \left( \prod_{m=1}^M \prod_{n=1}^N P(y_m(n); \lambda_m(n)) \right) \\ &= \sum_{m=1}^M \sum_{n=1}^N y_m(n) \log(\lambda_m(n)) - \lambda_m(n) - \log(y_m(n)!). \end{aligned}$$

## VI. EXPERIMENTS

### A. Data Preprocessing

We constructed the multivariate time series from text data as described in Section IV. The initial set of triples  $\mathcal{I}$  was collected from the articles published on the first and second day. For the dataset JS,  $|\mathcal{I}| = 1216$  and  $N = 44$ . For the dataset IP,  $|\mathcal{I}| = 570$  and  $N = 29$ . We also normalized  $y_{\text{append}}^{(i)}(n)$ ,  $y_{\text{extend}}^{(i)}(n)$ ,  $y_{\text{mutate}}^{(i)}(n)$  by their respective averages so they can be considered to be on the same scale.

Unlike a classic time-series setting where we have a single observed time-series, each triple in  $|\mathcal{I}|$  induces its only time-series  $\mathbf{y}^{(i)}(n)$ ,  $i \in \mathcal{I}$ . We assume that  $\mathbf{y}^{(i)}(n)$  is independent observations from the same stochastic process, which we will model as a discrete-time Hawkes process. However, this assumption is not true in our data.

We observed that time series induced by different initial triples can have very different dynamics. Therefore, to improve model fit, we applied K-means clustering algorithm with Euclidean distance to  $\mathbf{y}^{(i)}(n)$ ,  $i \in \mathcal{I}$  [24]. This decomposes the set of initial triples into  $K$  clusters:

$$\mathcal{I} = \mathcal{I}_1 \cup \mathcal{I}_2 \cup \dots \cup \mathcal{I}_K.$$

The discrete-time Hawkes process is then learned based on the time-series,  $\mathbf{y}^{(i)}(n)$ , induced by each cluster of initial triples. By analyzing the distribution of daily arrivals of the different change types, we decided on  $K = 3$ . For dataset JS, the number of initial triples in each cluster are  $|\mathcal{I}_1| = 155$ ,  $|\mathcal{I}_2| = 851$ ,  $|\mathcal{I}_3| = 210$ . For dataset IP, the number of initial triples in each cluster are  $|\mathcal{I}_1| = 127$ ,  $|\mathcal{I}_2| = 388$ ,  $|\mathcal{I}_3| = 55$ .

### B. RDF Graphs

Before we fit a dynamic model to the observed time-series, it is informative to consider why the different clusters have different dynamics. Figure 5 shows the three clusters of initial triples for datasets we collected as graphs. We will use the notation  $G^{(\mathcal{I}_1)}(1)$  to denote the RDF graph generated on day one from the triples in  $\mathcal{I}_1$ ;  $G^{(\mathcal{I}_2)}(1)$  to denote the RDF graph generated on day one from the triples in  $\mathcal{I}_2$ , etc. Table I and II show some representative words taken from the nodes of the corresponding RDF graphs. We can see that  $G^{(\mathcal{I}_1)}(1)$ ,  $G^{(\mathcal{I}_2)}(1)$ ,  $G^{(\mathcal{I}_3)}(1)$  are all topologically different.

The RDF graphs associated with  $G^{(\mathcal{I}_1)}(1)$  have a multi-hub structure. The hubs consist of important subject related to the news event such as *police*, *two man*, *actor* for dataset JS and *donald trump*, *united states*, *soleimani* for dataset IP. On the other hand,  $G^{(\mathcal{I}_2)}(1)$  is more decentralized and contains many isolated triples. As shown in Table I, these isolated triples tend

to reflect phrases that are tangentially (e.g., *jamal lyon*, *maga country*, *lee daniels*, *trump* for dataset JS and *state department*, *secretary mark esper* for dataset IP) related to the main subject. We can see that  $G^{(\mathcal{I}_3)}(1)$  are star networks. For the dataset JS, the central node is the phrase *jussie smollett*. For the dataset IP, the central node is the phrase *iran*.

TABLE I: Words Associated to the nodes of  $G^{(\mathcal{I}_k)}(1)$  in dataset JS

$\mathcal{I}_1$	$\mathcal{I}_2$	$\mathcal{I}_3$
police, two men, actor, attack, empire, surveillance video, hate crime, unknown chemical substance, racial homophobic slurs	actor, attack, empire, people, fox, jamal lyon, maga country, unknown chemical substance, racial homophobic slurs, lee daniels, trump	jussie smollett, two men, empire, northwestern memorial hospital, chicago, attackers

TABLE II: Words Associated to the nodes of  $G^{(\mathcal{I}_k)}(1)$  in dataset IP

$\mathcal{I}_1$	$\mathcal{I}_2$	$\mathcal{I}_3$
donald trump, united states, soleimani, people, officials, tehran, plane, strike	soleimani, attack, american troops, state department, iranian forces, iran supreme national security council, defence secretary mark esper, iran top general	iran, soleimani, sanctions, retaliation, baghdad, mahmoud ahmadinejad

### C. Model Fitting

To analyze how  $G^{(\mathcal{I}_1)}(1)$ ,  $G^{(\mathcal{I}_2)}(1)$ ,  $G^{(\mathcal{I}_3)}(1)$  change over time, we fit the induced time-series,  $\mathbf{y}^i(n)$ ,  $i \in \mathcal{I}_1$ ,  $\mathbf{y}^i(n)$ ,  $i \in \mathcal{I}_2$ ,  $\mathbf{y}^i(n)$ ,  $i \in \mathcal{I}_3$ , separately to the discrete-time Hawkes process introduced in Section V. This will inform us how the RDF graph sequences changes with append, extend, and mutate. We treated the time series induced by the  $i$ th triple as independent observations and solved for the maximum likelihood estimator,  $\hat{\Theta}$ , which included the  $3 \times 1$  baseline rate vector,  $\hat{\boldsymbol{\mu}} = [\hat{\mu}_{\text{append}}, \hat{\mu}_{\text{extend}}, \hat{\mu}_{\text{mutate}}]^T$  and the  $3 \times 3$  infectivity matrix,  $\hat{\mathbf{A}}$ . We set the hyperparameter  $\beta$  in (3) to 2.

Let  $\hat{\boldsymbol{\mu}}^{(\mathcal{I}_k)}$  denote the baseline rate vector estimated from  $\mathbf{y}^i(n)$ ,  $i \in \mathcal{I}_k$ . Table III shows the estimated value for the three clusters. We can see that the estimated baseline rate differs amongst  $G^{(\mathcal{I}_1)}(1)$ ,  $G^{(\mathcal{I}_2)}(1)$ ,  $G^{(\mathcal{I}_3)}(1)$ .

TABLE III: Baseline Rate Vector Estimate

Dataset		$\hat{\boldsymbol{\mu}}^{(\mathcal{I}_1)}$	$\hat{\boldsymbol{\mu}}^{(\mathcal{I}_2)}$	$\hat{\boldsymbol{\mu}}^{(\mathcal{I}_3)}$
JS	Append	0.2194	0.145	1.0456
	Extend	0.5553	0.0655	0.9762
	Mutate	0.0836	0.0056	0.1243
IP	Append	1.0971	0.2759	1.3088
	Extend	0.7171	0.1013	1.1393
	Mutate	0.1692	0.0363	0.7686

In general, we see that the baseline rate for append is higher than the rate for extend and mutate. This means new

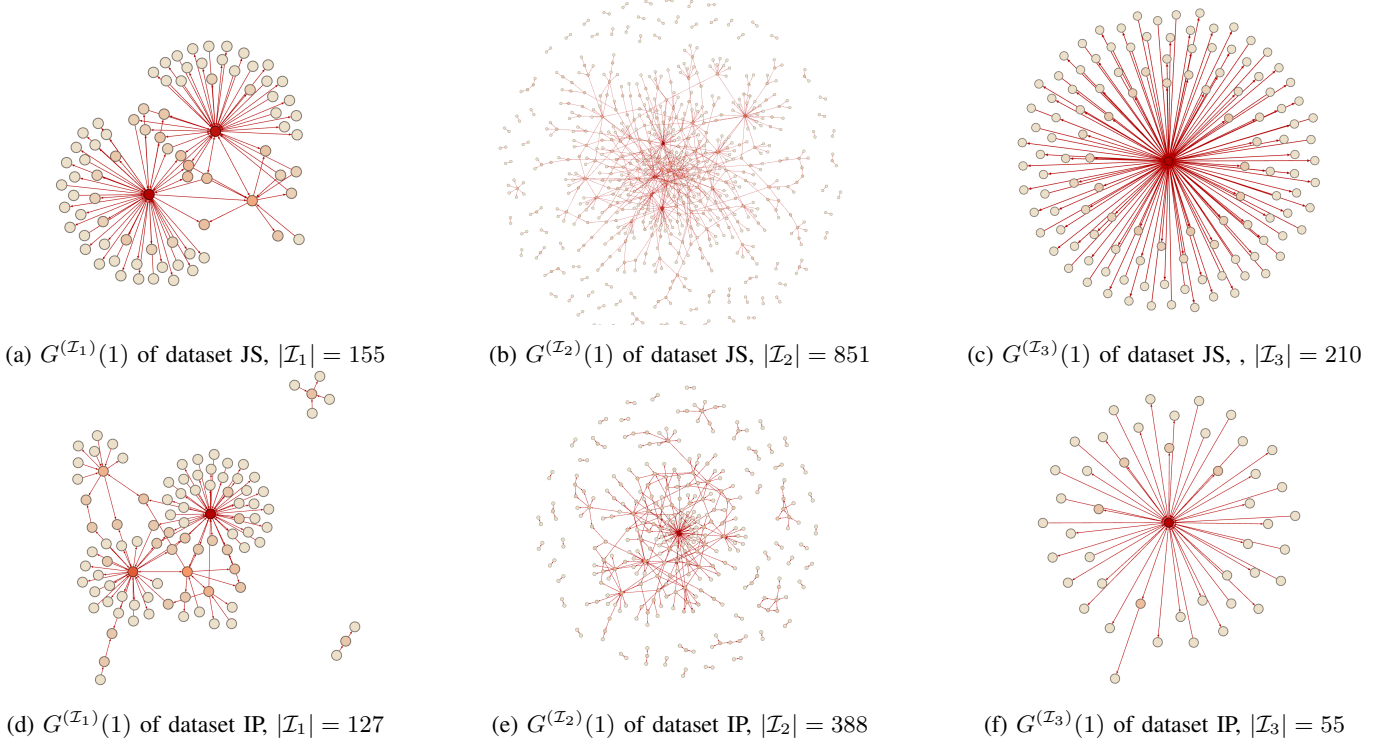


Fig. 5: RDF graphs constructed from different set of initial triples (words and multi-edges are removed)

information is being reported and that the corresponding RDF graph sequence  $G^{(\mathcal{I}_k)}$  is growing larger with more nodes and edges. We see that the rate for append is the largest for  $G^{(\mathcal{I}_3)}(1)$  compared to  $G^{(\mathcal{I}_1)}(1)$  and  $G^{(\mathcal{I}_2)}(1)$ . This is because  $G^{(\mathcal{I}_3)}(1)$  is a star-network whose hub node is the main keyword of the news event. Therefore, as additional news events get reported, new information (i.e., triples) will be appended to the hub node.

Let  $\hat{\mathbf{A}}^{(\mathcal{I}_k)}$  denote the baseline infectivity matrix estimated from  $\mathbf{y}^i(n)$ ,  $i \in \mathcal{I}_k$ . The  $(i, j)$ th entry of the infectivity matrix,  $\hat{\mathbf{A}}^{(\mathcal{I}_k)}$ , indicates a change of type  $j$  can affect a change of type  $i$ . Figure 6 shows the estimated infectivity matrix for both datasets. We can see that the infectivity matrix is not a symmetric matrix.

The value of  $\hat{\mathbf{A}}_{\text{extend,append}}^{(\mathcal{I}_k)}$  is larger than  $\hat{\mathbf{A}}_{\text{append,extend}}^{(\mathcal{I}_k)}$ . This means that when there are more append changes, there will be more extend changes to  $G^{(\mathcal{I}_k)}$  over time. We can consider extend changes as drawing connection between separate concepts (i.e., triples) and append changes as adding new information. This shows that making the addition of new information often leads to more connection between concepts. However, the connection between past concepts does not necessarily motivate new information.

We see that  $\hat{\mathbf{A}}_{\text{extend,mutate}}^{(\mathcal{I}_k)}$  is much larger than  $\hat{\mathbf{A}}_{\text{mutate,extend}}^{(\mathcal{I}_k)}$ . This means that occurrences of mutate changes (i.e., different ways of stating the same information) lead to more extend changes (i.e., making connections between concepts) but not the other way around. Similarly,  $\hat{\mathbf{A}}_{\text{append,mutate}}^{(\mathcal{I}_k)}$  is larger than  $\hat{\mathbf{A}}_{\text{mutate,append}}^{(\mathcal{I}_k)}$ . This shows occurrences of mutate changes also

lead to more append change changes. Roughly, we can infer that in news articles, the diversity of sentence patterns (i.e., mutate) contains both new information and novel connection. However, new information does not indicate diversity in sentence patterns. Given  $\hat{\mu}^{(\mathcal{I}_k)}$  and  $\hat{\mathbf{A}}^{(\mathcal{I}_k)}$ , we can use equation (2) to find  $\hat{\lambda}^{(i)}(n)$ ,  $i \in \mathcal{I}_k$ , which is the expected number of occurrences of append, extend, and mutate per time unit. Figure 7 plots the average value over all the induced time-series

$$\overline{\lambda^{(\mathcal{I}_k)}}(n) = \frac{1}{|\mathcal{I}_k|} \sum_{i \in \mathcal{I}_k} \hat{\lambda}^{(i)}(n).$$

We can see that the rate of mutate is the smallest compared with append and extend in  $G^{(\mathcal{I}_2)}(1)$ , particularly for dataset JS. This is further evidence that  $G^{(\mathcal{I}_2)}(1)$  grows differently from  $G^{(\mathcal{I}_1)}(1)$  and  $G^{(\mathcal{I}_3)}(1)$ . The reason is that the triples of  $G^{(\mathcal{I}_2)}(1)$  are typically phrases that are only tangentially related to the primary news event.

#### D. Forecasting

In this section, we use the discrete-time Hawkes process (built from training data from  $n = 1 \dots N$ ) to predict how the RDF graphs,  $G^{(\mathcal{I}_k)}(1)$ , will evolve in the future using equations (2) and (4). The predicted value at time  $N + 1$  is



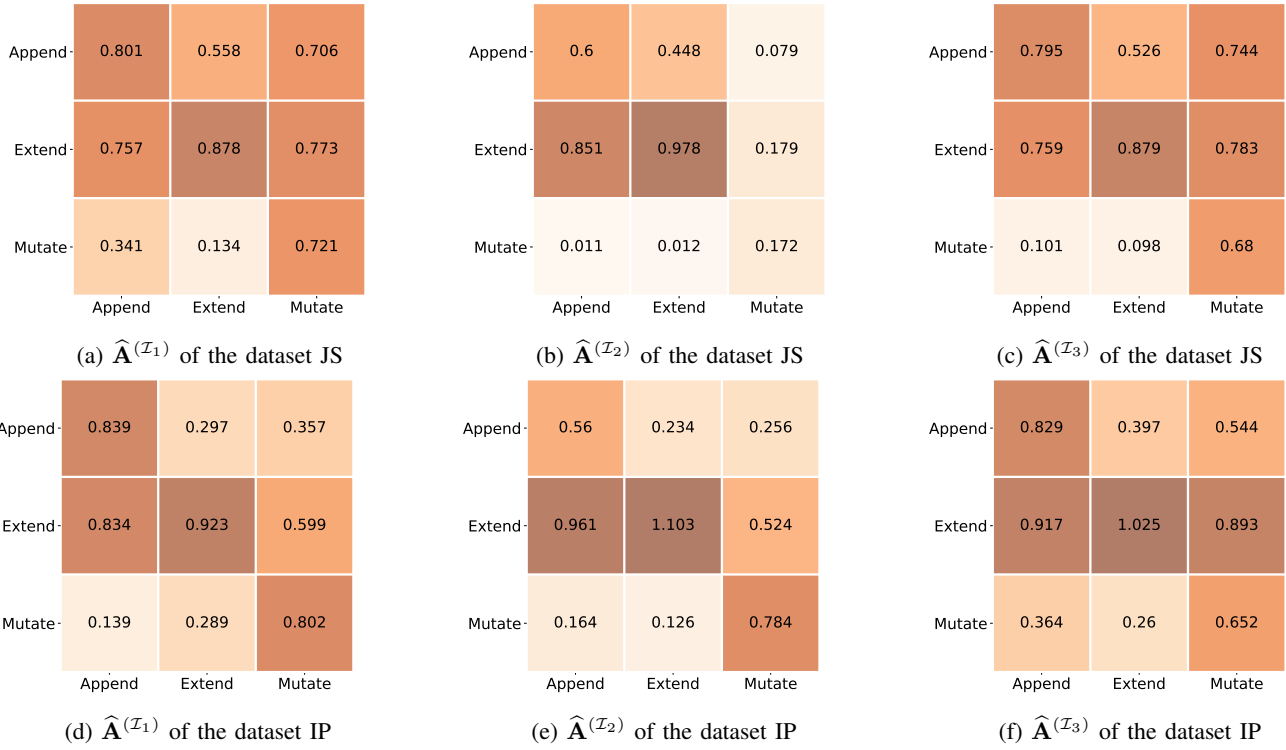


Fig. 6: Infectivity Matrix Estimate

TABLE IV: SMAPE Forecasting Results

Dataset		Method	No Clustering	$\overline{e^{(\mathcal{I}_1)}}$	$\overline{e^{(\mathcal{I}_2)}}$	$\overline{e^{(\mathcal{I}_3)}}$	$\text{avg}(\overline{e^{(\mathcal{I}_1)}}, \overline{e^{(\mathcal{I}_2)}}, \overline{e^{(\mathcal{I}_3)}})$
JS	Append	VAR	176.6%	142.9%	190.2%	167.7%	166.9%
		LSTNet	177.5%	174.3%	179.4%	180.6%	178.1%
		DHP	167.7%	155.6%	190.1%	148.4%	164.7%
	Extend	VAR	128.8%	80.4%	133.7%	70.8%	95.0%
		LSTNet	133.8%	127.0%	134.5%	129.2%	130.2%
		DHP	132.6%	68.6%	144.8%	87.0%	100.1%
	Mutate	VAR	193.4%	183.9%	190.6%	175.2%	183.2%
		LSTNet	194.2%	191.3%	191.7%	193.5%	192.2%
		DHP	195.3%	188.6%	193.1%	185.7%	189.1%
IP	Append	VAR	181.7%	146.7%	193.2%	158.5%	166.1%
		LSTNet	187.7%	158.9%	193.9%	189.6%	180.8%
		DHP	178.6%	148.5%	193.2%	171.9%	171.2%
	Extend	VAR	138.1%	120.0%	159.6%	100.7%	126.8%
		LSTNet	147.3%	122.4%	157.0%	82.6%	120.7%
		DHP	153.6%	125.5%	151.7%	90.4%	122.5%
	Mutate	VAR	198.1%	199.4%	196.9%	199.4%	198.6%
		LSTNet	198.9%	199.3%	196.2%	199.8%	198.4%
		DHP	199.7%	199.5%	199.8%	197.7%	199.0%

then

$$\begin{aligned}
\hat{\mathbf{y}}^{(i)}(N+1) &= \max_{\mathbf{y}^{(i)}(N+1)} P(\mathbf{y}^{(i)}(N+1); \hat{\lambda}^{(i)}(N+1)) \\
&= \hat{\lambda}^{(i)}(N+1) \\
&= \hat{\mu} + \sum_{t < N} \hat{\mathbf{A}} \mathbf{y}^{(i)}(t) \phi(N-t), \quad i \in \mathcal{I}
\end{aligned}$$

We compare the predicted value using the discrete-time Hawkes process (DHP) with two state-of-the-art multivariate time series models: vector autoregression (VAR) [2] and long and short-term time-series network (LSTNet) [3]. We evaluate

the error between the predicted value and the observed value using Symmetric Mean Absolute Percentage Error (SMAPE). The advantages of SMAPE are 1) it does not depend on the scale of the observations; 2) it has a lower (0%) and upper (200%) bound

$$e(\mathbf{y}^{(i)}, \hat{\mathbf{y}}^{(i)}) = 200 \frac{|\mathbf{y}^{(i)}(N+1) - \hat{\mathbf{y}}^{(i)}(N+1)|}{|\mathbf{y}^{(i)}(N+1)| + |\hat{\mathbf{y}}^{(i)}(N+1)|}, \quad i \in \mathcal{I}.$$

We computed the SMAPE for  $\hat{\mathbf{y}}^{(i)}(N+1)$  with and without decomposing the set of initial triples  $\mathcal{I}$  into three clusters.

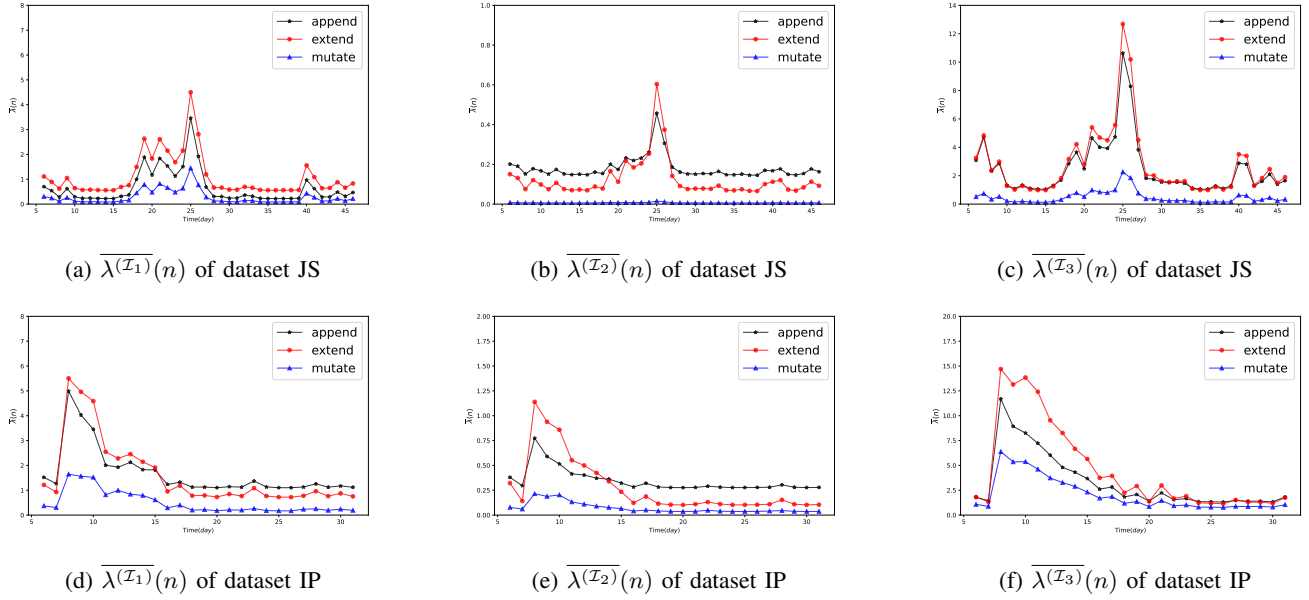


Fig. 7: Average Conditional Intensity Function  $\overline{\lambda(\mathcal{I}_k)}(n)$

Since each triple from  $\mathcal{I}$  induced its own time-series, we found the average error over all the triples

$$\overline{e(\mathcal{I}_k)} = \frac{1}{|\mathcal{I}_k|} \sum_{i \in \mathcal{I}_k} e(\mathbf{y}^{(i)}, \hat{\mathbf{y}}^{(i)}).$$

Table IV shows the average SMAPE for  $\hat{\mathbf{y}}^{(i)}(N+1)$  with 5-fold cross-validation (i.e., we predict  $\hat{\mathbf{y}}^{(i)}(N+1)$  for 5 different  $N$  values). The forecasting results are comparable between all three methods; one additional advantage of DHP is that the parameters are interpretable. We can see errors are generally smaller if we decompose the set of initial triples into clusters first. This is due to the complex dynamics of how the RDF graph changes over time.

## VII. CONCLUSION

We proposed a framework of converting a corpus of news articles collected over time to a sequence of RDF graphs using semantic triples extraction. It is very challenging to model dynamic graphs. Therefore, we considered an approximation by using multivariate time series, which kept track of three types of topological changes to the initial triples in the sequence of RDF graphs: append, extend, mutate. We then fit the time series using discrete-time Hawkes process. Analyzing the RDF graphs can give us insights to the semantic content from the original articles while the dynamic parameters of the Hawkes process give us insight to how the semantic content evolves over time.

For future work, we will do more analysis on the structural properties of the RDF graph and their relationship to the semantic content of news. Several independence assumptions were made to simplify the process of fitting observed data to the discrete-time Hawkes process; we will investigate more

complicated models that make less assumptions about statistical independence.

## ACKNOWLEDGMENT

This work was funded in part by the Defense Advanced Research Projects Agency (DARPA) Active Interpretation of Disparate Alternatives (AIDA) Program under Air Force Research Laboratory (AFRL) prime contract no. FA8750-19-2-0027. Any opinions, findings, and conclusion or recommendations expressed in this material are those of the authors and do not necessarily reflect the view of the DARPA, AFRL, or the US government. This work was also partially supported by the National Science Foundation AI Institute in Dynamic Systems (Grant No. 2112085)

## REFERENCES

- [1] A. Fader, S. Soderland, and O. Etzioni, "Identifying relations for open information extraction," in *Proceedings of the 2011 conference on empirical methods in natural language processing*, 2011, pp. 1535–1545.
- [2] H. Lütkepohl, *New introduction to multiple time series analysis*. Springer Science & Business Media, 2005.
- [3] G. Lai, W.-C. Chang, Y. Yang, and H. Liu, "Modeling long- and short-term temporal patterns with deep neural networks," in *The 41st International ACM SIGIR Conference on Research & Development in Information Retrieval*, 2018, pp. 95–104.
- [4] J. Allan, J. G. Carbonell, G. Doddington, J. Yamron, and Y. Yang, "Topic detection and tracking pilot study final report," 1998.
- [5] J. Allan, R. Papka, and V. Lavrenko, "On-line new event detection and tracking," in *Proceedings of the 21st annual international ACM SIGIR conference on Research and development in information retrieval*, 1998, pp. 37–45.
- [6] D. G. Ghalandari and G. Ifrim, "Examining the state-of-the-art in news timeline summarization," *arXiv preprint arXiv:2005.10107*, 2020.
- [7] T. Brants, F. Chen, and A. Farahat, "A system for new event detection," in *Proceedings of the 26th annual international ACM SIGIR conference on Research and development in information retrieval*, 2003, pp. 330–337.



- [8] Q. Zhao, P. Mitra, and B. Chen, "Temporal and information flow based event detection from social text streams," in *AAAI*, vol. 7, 2007, pp. 1501–1506.
- [9] R. Nallapati, A. Feng, F. Peng, and J. Allan, "Event threading within news topics," in *Proceedings of the thirteenth ACM international conference on Information and knowledge management*, 2004, pp. 446–453.
- [10] B. Liu, F. X. Han, D. Niu, L. Kong, K. Lai, and Y. Xu, "Story forest: Extracting events and telling stories from breaking news," *ACM Transactions on Knowledge Discovery from Data (TKDD)*, vol. 14, no. 3, pp. 1–28, 2020.
- [11] Q. Mei and C. Zhai, "Discovering evolutionary theme patterns from text: an exploration of temporal text mining," in *Proceedings of the eleventh ACM SIGKDD international conference on Knowledge discovery in data mining*, 2005, pp. 198–207.
- [12] A. Das Sarma, A. Jain, and C. Yu, "Dynamic relationship and event discovery," in *Proceedings of the fourth ACM international conference on Web search and data mining*, 2011, pp. 207–216.
- [13] C. C. Yang, X. Shi, and C.-P. Wei, "Discovering event evolution graphs from news corpora," *IEEE Transactions on Systems, Man, and Cybernetics-Part A: Systems and Humans*, vol. 39, no. 4, pp. 850–863, 2009.
- [14] A. Spitz, S. Almasian, and M. Gertz, "Topexnet: entity-centric network topic exploration in news streams," in *Proceedings of the twelfth ACM international conference on web search and data mining*, 2019, pp. 798–801.
- [15] A. G. Hawkes, "Spectra of some self-exciting and mutually exciting point processes," *Biometrika.*, vol. 58, no. 1, 1971.
- [16] R. Kobayashi and R. Lambiotte, "Tideh: Time-dependent hawkes process for predicting retweet dynamics," in *Tenth International AAAI Conference on Web and Social Media*, 2016.
- [17] M. Farajtabar, Y. Wang, M. Gomez-Rodriguez, S. Li, H. Zha, and L. Song, "Coevolve: A joint point process model for information diffusion and network evolution," *The Journal of Machine Learning Research*, vol. 18, no. 1, pp. 1305–1353, 2017.
- [18] H. S. Dutta, V. R. Dutta, A. Adhikary, and T. Chakraborty, "Hawkeseye: Detecting fake retweeters using hawkes process and topic modeling," *IEEE Transactions on Information Forensics and Security*, vol. 15, pp. 2667–2678, 2020.
- [19] "eventregistry." [Online]. Available: <https://eventregistry.org/>
- [20] "Neuralcoref 4.0: Coreference resolution in spacy with neural networks." [Online]. Available: <https://github.com/huggingface/neuralcoref>
- [21] "spacy: Industrial-strength nlp." [Online]. Available: <https://github.com/explosion/spaCy>
- [22] T. Mikolov, I. Sutskever, K. Chen, G. S. Corrado, and J. Dean, "Distributed representations of words and phrases and their compositionality," in *Advances in neural information processing systems*, 2013, pp. 3111–3119.
- [23] R. Browning, D. Sulem, K. Mengersen, V. Rivoirard, and J. Rousseau, "Simple discrete-time self-exciting models can describe complex dynamic processes: A case study of covid-19," *Biometrika.*, vol. 16, no. 1, 2021.
- [24] S. Aghabozorgi, A. S. Shirkhorshidi, and T. Y. Wah, "Time-series clustering—a decade review," *Information Systems*, vol. 53, pp. 16–38, 2015.